PCCP

Accepted Manuscript

PCCP

PAPER

Structural change of $NaO_{1/2}$-WO_3-$NbO_{5/2}$-$LaO_{3/2}$-$PO_{5/2}$ glass induced by electrochemical substitution of sodium ions with protons

Tomohiro Ishiyama,[a, †] **Takuya Yamaguchi,**[a] **Junji Nishii,**[b] **Toshiharu Yamashita,**[c] **Hiroshi Kawazoe,**[c] **Naoaki Kuwata,**[d] **Junichi Kawamura**[d] **and Takahisa Omata**[* a]

Structural changes of $35NaO_{1/2}$-$1WO_3$-$8NbO_{5/2}$-$5LaO_{3/2}$-$51PO_{5/2}$ glass (1W-glass) before and after the electrochemical substitution of sodium ions with protons by alkali-proton substitution (APS) are studied by Raman and ^{31}P magic-angle spinning nuclear magnetic resonance (MAS-NMR) spectroscopies. The
10 glass before APS consists of $(PO_3^-)_{8.6}(P_2O_7^{4-})$ chains on average and the terminal Q^1 units (-O-PO_3^{3-}) are bound to MO_6 octahedra (M denotes niobium or tungsten) through P-O-M bonds. Some non-bridging oxygens (NBOs) in the MO_6 octahedra are present in addition to the bridging oxygens (BOs) in P-O-M bonds. APS induces fragmentation of the phosphate chains because the average chain length decreases to $(PO_3^-)_{3.7}(P_2O_7^{4-})$ after APS, despite the total number of modifier cations of sodium and lanthanum ions
15 and protons being unaffected by APS. This fragmentation is induced by some of the NBOs in the MO_6 octahedra before APS changing to BOs of the newly formed M-O-P bonds after APS because of the preferential formation of P-OH bonds over M-OH ones in the present glass. We show that APS under the conditions used here is not a simple substitution of sodium ions with protons, but is accompanied by structural relaxation of the glass to stabilize the injected protons.

20 1. Introduction

Fuel cells that operate in the intermediate temperature region of 300–500 °C, termed intermediate-temperature fuel cells (IT-FCs), attract considerable attention because of their advantages in terms of cost, energy efficiency and operating conditions.[1-3] In addition,
25 their operating temperature enables use of a variety of fuels such as hydrocarbons and alcohols. Therefore, many research groups have focused on developing solid electrolytes applicable to IT-FCs by attempting to identify solid proton conductors that show sufficiently high conductivity at intermediate temperatures.[4-13]
30 However, such a material has not been developed yet.

Glass has been studied as an electrolyte material for a long time because of its variety of compositions and high chemical and electrochemical durability. For example, a glass electrolyte with high lithium (Li)-ion conductivity has recently been developed as
35 a material for solid-state Li-ion batteries.[14-16] Proton-conducting glass electrolytes applicable to IT-FCs have also been studied; however, it is difficult to maintain highly concentrated protons in glass at intermediate temperatures. Generally, the proton concentration in phosphate glass prepared by the conventional
40 melt-quenching method is in the order of 10^{19} cm^{-3}.[17] While the proton concentration in glass prepared by the sol-gel method is up to 10^{21} cm^{-3} at room temperature, the protons are usually exhausted at temperatures higher than 200 °C because of dehydration.[18]
45 We recently developed a technique termed alkali-proton

substitution (APS) to inject carrier protons into oxide glass by the electrochemical substitution of alkali ions in the glass with protons at high temperatures.[11-13] This technique enables injection of carrier protons with a concentration exceeding $5×10^{21}$ cm^{-3},
50 which corresponds to a concentration higher than ~10 mol L^{-1}. The carrier protons injected by APS are stably maintained at temperatures above 300 °C because APS is usually conducted at temperatures in the range of 300–500 °C, which are much higher than the temperatures employed for ion exchange using aqueous
55 acid solution.[19-21] For example, the carrier protons injected in $35NaO_{1/2}$-$1WO_3$-$8NbO_{5/2}$-$5LaO_{3/2}$-$51PO_{5/2}$ glass (1W-glass) by APS are stable up to 300 °C. Therefore, the APS technique allowing injection of highly concentrated proton carriers that are stable at intermediate temperatures is very attractive to realize
60 proton-conducting glass electrolytes suitable for IT-FCs, although the proton conductivity of the 1W-glass after APS was not sufficiently high ($4 × 10^{-4}$ Scm^{-1} at 250 °C) and should be improved.

In our previous paper, we studied the substitution behavior
65 during APS of 1W-glass in terms of the quantity and macroscopic distribution of injected protons using energy-dispersive X-ray (EDX) and infrared (IR) spectroscopies.[13] We found that protons were injected into the region of the glass where the concentration of sodium ions (Na$^+$) had decreased, and the amounts of
70 injected protons and discharged Na$^+$ ions were equivalent. Macroscopically, this indicates that the Na$^+$ ions in the glass were substituted with protons. Microscopically, *i.e.*, in terms of atomic arrangement, we observed that APS developed without

crystallization, phase separation and the other significant structural changes in the network structure by Raman spectroscopy. The character of the chemical bond of the proton with the oxygen is evidently different from that of Na^+ ion with the non-bridging oxygen (NBO) in the glass network. This implies the difference in the atomic arrangement, i.e., structure, of the glass before and after APS, although the substitution of Na^+ ions with protons by APS in macroscopic scale was confirmed.

Recently, we reported that glass composition that determines glass structure has a huge effect on the mobility of proton carriers.[22] Consequently, to understand the structure of the glass before and after APS is very important to design the glass composition that realizes high proton conductivity. On the other hand, the WO_3 and $NbO_{5/2}$ that exhibit intermediate components of glass former and modifier raise the glass transition temperature and increase thermal stability. Therefore, to understand how the WO_3 and $NbO_{5/2}$ are involved in the glass network should provide important information in order to improve thermal stability of the proton conducting glass.

Based on this situation, we studied the structure of 1W-glass before and after APS in detail by ^{31}P magic-angle spinning nuclear magnetic resonance (MAS-NMR) spectroscopy in addition to Raman spectroscopy in order to obtain structural information about the degree of polymerization of phosphate network quantitatively.

2. Experimental

2.1. Glass preparation

Glass with a composition of $35NaO_{1/2}$-$1WO_3$-$8NbO_{5/2}$-$5LaO_{3/2}$-$51PO_{5/2}$ (1W-glass) was prepared by the conventional melt-quenching technique. Raw materials Na_2CO_3, WO_3, Nb_2O_5, La_2O_3 and H_3PO_4 were weighed and mixed, and then melted in a platinum crucible for 1 h at 1400 °C in air. The molten materials were poured into a cylindrical carbon mold with an inner diameter of 18 mm, annealed at 420 °C for 10 min and then cooled slowly to room temperature in the furnace at a cooling rate of 20 °C h^{-1}. The glass transition temperature of the glass was determined to be 415 °C by differential thermal analysis (TG/DTA6300, SII, Japan).

2.2. Alkali-proton substitution

APS was performed on the 1W-glass using an APS apparatus (KDK-800, Kenix Co., Japan). The configuration of this apparatus was described in our previous paper.[12] Disk-shaped glass plates with a diameter of 18 mm and thickness of 1 mm were sliced from the cylindrical glass block and both surfaces were polished. A thin film of palladium (Pd) with a thickness of approximately 0.2 μm was deposited by magnetron sputtering on one surface of the glass plate. The glass plate was then positioned in a holder made of quartz with the Pd-deposited surface facing upwards. The other face of the glass was placed in contact with molten tin (Sn) heated at 310 °C under 5% H_2/95% N_2 atmosphere. A DC bias of 5.0 V was applied between the Pd anode and molten Sn cathode for 7 or 30 h. The electrochemical substitution of Na^+ ions with protons was completed for the glass after APS for 30 h, but was not after 7 h, as described in our previous paper.[13]

2.3. Structural characterization

Raman spectra of the glasses before and after APS were measured using an NRS-3100 laser Raman spectrometer (JASCO, Japan) at an excitation wavelength of 532 nm. Cross-sectional Raman spectra of the glass after 7 h of APS were measured at 50-μm intervals along the direction from anode to cathode.

^{31}P MAS-NMR spectra of the glasses before and after 30 h of APS were acquired on a Bruker Avance 600 spectrometer (Bruker BioSpin, Germany) operating at 14.1 T (Larmor frequency of 242.92 MHz) with a 2.5-mm magic-angle spinning probe operating at a spinning frequency of 30 kHz. The spectra were acquired using a pulse length of 4 μs (90° flip angle) and recycle delay of 10 s; the spectra were referenced relative to 85% H_3PO_4 by setting the signal of solid $(NH_4)_2HPO_4$ to 1.33 ppm. The obtained signals were deconvoluted in the range from 20 to -60 ppm into two or three pseudo-Voigt functions using DMfit.[23]
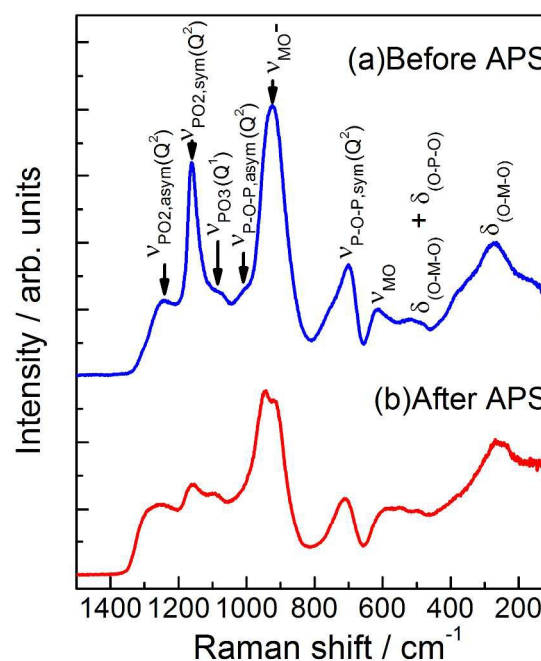
3. Results

Fig.1 Raman spectra of 1W-glass (a) before and (b) after APS for 30 h.

3.1. Raman spectra

Figure 1(a) shows a Raman spectrum of 1W-glass before APS. The bands at 200–400 cm^{-1} are associated with the bending modes of O-M-O ($\delta_{O\text{-}M\text{-}O}$; M denotes niobium (Nb) or tungsten (W)) of MO_6 octahedra, and the band at ~500 cm^{-1} is their combination modes with an O-P-O bending mode ($\delta_{O\text{-}P\text{-}O}$; P is phosphorus).[24-27] The bands at ~600 and 924 cm^{-1} are also associated with the MO_6 octahedra. That at lower frequency is assigned to the stretching mode for the long M-O bonds (ν_{MO}); i.e., related to M-O-P or M-O-M bonds with bridging oxygen (BO). The band at 924 cm^{-1} is assigned to a stretching mode of short M-O bonds where O does not bridge between a P and Nb or W atom; this mode is indicated as ν_{MO}-. The remaining bands are associated with the stretching modes of the phosphate framework.

It is well known that the frequency of these stretching modes depends on the polymerization level of PO_4 tetrahedra; this is usually represented by the number of P-O-P linkages, n, $i.e.$, the number of BOs, of an individual PO_4 tetrahedron as Q^n (n=0, 1, 2 and 3).[28] Using this notation, the bands observed at 700 and 1016 cm^{-1} are assigned to the symmetric and asymmetric stretching modes of P-O-P, respectively, indicated by $\nu_{P-O-P,sym}(Q^2)$ and $\nu_{P-O-P,asym}(Q^2)$ for Q^2 units, respectively.[28-30] The bands located at higher wavenumber than 1050 cm^{-1} are associated with the stretching mode of P-O⁻ bonds related to NBO; the band at 1080 cm^{-1} is assigned to that for the Q^1 unit, $\nu_{PO3}(Q^1)$. The bands at 1162 and 1248 cm^{-1} are respectively assigned to the symmetric and asymmetric modes for the Q^2 unit; $i.e.$, $\nu_{PO2,sym}(Q^2)$ and $\nu_{PO2,asym}(Q^2)$, respectively.[28-30] These assignments are summarized in Table 1.

Figure 1(b) shows the Raman spectrum of the glass after APS for 30 h. Sodium and proton concentrations are not dependent on the position in this glass, because the substitution of sodium ions with protons was completed within the 30 h; therefore, the Raman spectra do not vary along the direction from anode to cathode in this glass. The spectral shape is similar to those of the glass before APS; however, the positions and intensities of the bands are slightly changed compared to those of the glass before APS.

Table 1 Assignment of the Raman bands observed for 1W-glass before and after APS.

Frequency (cm^{-1})		Assignment*	Ref.
Before APS	After APS		
270	270	δ_{O-M-O}　Bending mode of O-M-O of MO_6 octahedra	24–27
378	378	δ_{O-M-O^-}　Bending mode of O-M-O⁻ of MO_6 octahedra	24–27
523	523	$\delta_{O-M-O} + \delta_{O-P-O}$　Combination mode of O-M-O bending mode with O-P-O bending mode	24–27
614	614	ν_{MO}　Stretching mode of M-O bond of MO_6 octahedra	24–27
700	720	$\nu_{P-O-P,sym}(Q^2)$　Symmetric stretching mode of P-O-P bond for Q^2 unit	28–30
924	920	ν_{MO^-}　Stretching mode of M-O⁻ bond of MO_6 octahedra	24–27
-	950	ν_{MO^-}　Stretching mode of M-O⁻ bond of MO_6 octahedra. The number of NBO in a MO_6 octahedra for this band is smaller than that for the 920 cm^{-1} band.	
1016	1016	$\nu_{P-O-P,asym}(Q^2)$　Asymmetric stretching mode of P-O-P bond for Q^2 unit.	28, 30
1080	1080	$\nu_{PO3}(Q^1)$　Symmetric stretching mode of NBOs for Q^1 unit	28, 30
1162	1162	$\nu_{PO2,sym}(Q^2)$　Symmetric stretching mode of NBOs for Q^2 unit	28–30
1248	1248	$\nu_{PO2,asym}(Q^2)$　Asymmetric stretching mode of NBOs for Q^2 unit	28–30

*M denotes Nb or W.

To clarify these spectral changes, we measured Raman spectra at different depths in the 1W-glass to determine the level of APS. Figure 2(a) shows the Na and hydroxide (OH) concentration profiles of 1W-glass after APS for 7 h measured for the cross section along the direction from anode to cathode. Na and OH concentrations at a distance from the Pd anode x of 0.6–1.0 mm were almost identical to those of the glass before APS. At distances of 0–0.5 mm from the Pd anode, the Na concentration decreased and OH concentration increased approaching the anode. This indicates that the level of APS increased closer to the anode in the range of x=0–0.5 mm.

Raman spectra of the same region as in Fig. 2(a) are depicted in Fig. 2(b). The spectral shape for the region of x=0.5–0.9 mm is identical to that of the glass before APS as expected, because APS did not occur in this region (see Fig. 2(a)). In the region of x=0.45–0.05 mm, the spectral shape depended on x. The most characteristic change associated with the phosphate framework is the shift of the $\nu_{P-O-P,sym}(Q^2)$ band at ~700 cm^{-1}. This band shifted to higher frequency closer to the anode; $i.e.$, it shifted to higher frequency as the substitution of Na⁺ ions with protons increased. This shift of the $\nu_{P-O-P,sym}(Q^2)$ band is attributed to the decrease of length, that is, fragmentation, of phosphate chains consisting of inner Q^2 units and two terminal Q^1 units; $i.e.$, $(PO_3^-)_m(P_2O_7^{4-})$.[31]

Another change associated with the phosphate framework is variation of intensity of the $\nu_{PO2,sym}(Q^2)$ band at 1162 cm^{-1}, which decreased in intensity markedly as the substitution level of Na⁺ ions with protons increased. This may be because the polarizability of protons is much smaller than that of Na⁺ ions taking into account that the intensity of the Raman band is determined by the change in polarizability.[32-34]

For the bands related to MO_6 octahedra, the ν_{M-O^-} band that appeared to be a singlet before APS split into a doublet after APS, and the intensity of the band at 950 cm^{-1} increased with substitution level. According to Fukumi $et\ al.$,[25] the ν_{Nb-O^-} band shifts to higher frequency as the number of NBOs in each NbO_6 octahedron decreases. Therefore, the spectral change around 900–950 cm^{-1} indicates that the number of NBOs in each MO_6 octahedron decreased with increasing substitution level. This means that new M-O-P (or M-O-M) bonds were formed during APS by consumption of some of the NBOs in the MO_6 octahedra.

3.2. NMR spectra

Figure 3(a) shows a ³¹P MAS-NMR spectrum of the glass before APS. A signal appears between 5 and -40 ppm that can be assigned to Q^1 or Q^2 units based on their chemical shifts.[35] This indicates that no Q^0 or Q^3 units, $i.e.$, orthophosphate or

ultraphosphate ions, are present in the glass, consistent with the results obtained from Raman spectroscopy. Consequently, the glass before APS contains $(PO_3^-)_m(P_2O_7^{4-})$ chains. Because the spectrum is broad and obviously asymmetric, it was deconvoluted

5 into three signals at 1.4, -10.8 and -20.9 ppm, as indicated by thin solid lines in Fig. 3(a). The signals at 1.4 and -20.9 ppm can be attributed to Q^1 and Q^2 units, respectively.[35] The signal at -10.8 ppm is attributable to a Q^1 unit in which one of the three NBO bonds to Nb or W form a single P–O–M linkage;[36] hereafter, this
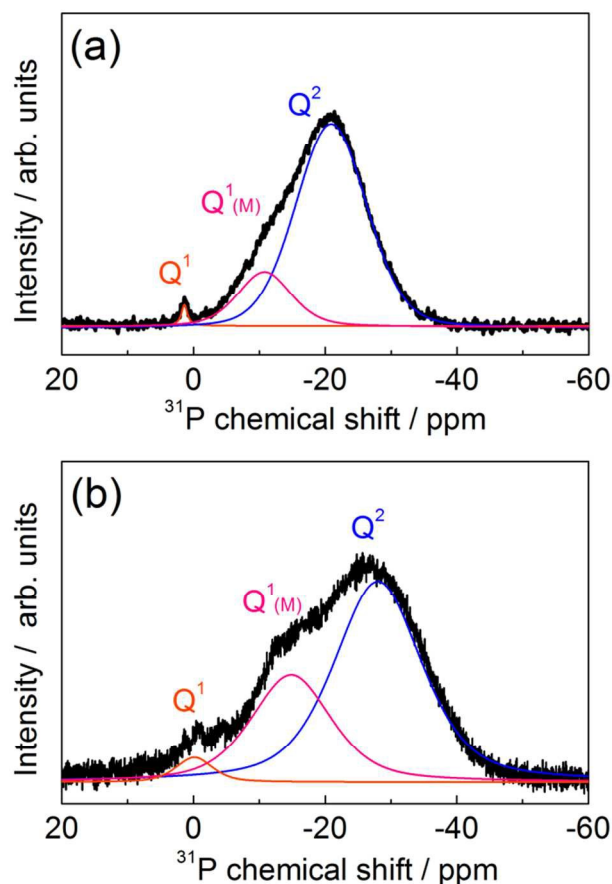
10 type of PO_4 tetrahedron is termed $Q^1_{(M)}$.

Figure 3(b) shows a ^{31}P MAS-NMR spectrum of the glass after APS for 30 h. The spectral shape is very similar to that of the glass before APS (Fig. 3(a)), but the signals are shifted upfield by
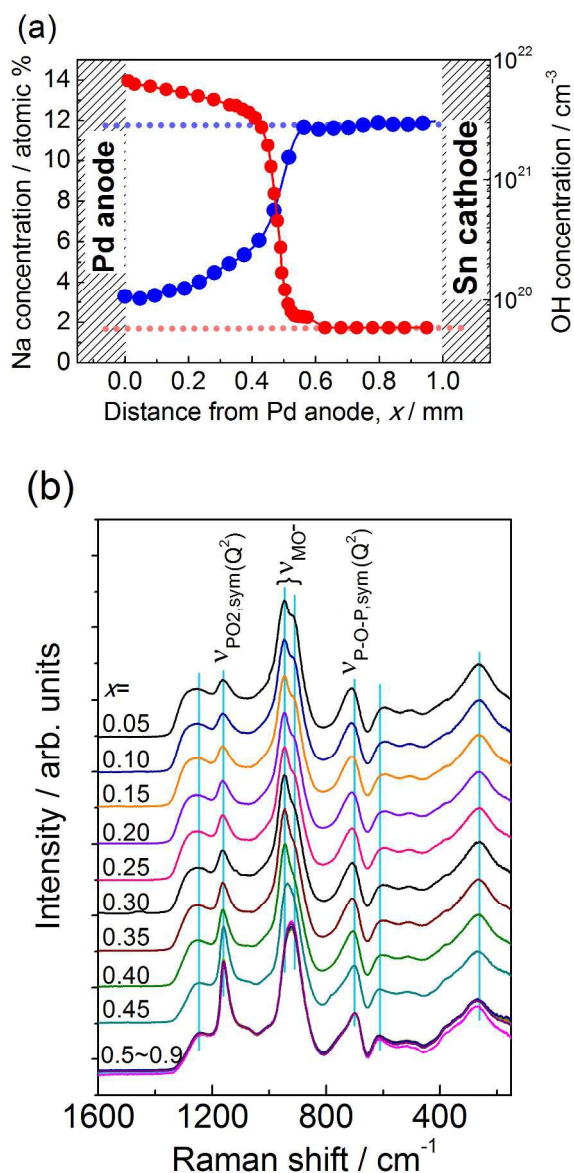
5–10 ppm. The upfield shift of the spectrum of the glass after APS can be explained as follows. The ^{31}P chemical shift of phosphate glass depends on not only the polymerization level of PO_4 tetrahedra, i.e., the value n of Q^n, but also the species of

25 modifier cations. For example, the ^{31}P NMR signal of $(Li_xNa_{1-x})PO_3$ glasses shifted upfield with increasing Li concentration.[35] Such dependence on the species of modifier cation has been studied for various phosphate glasses by Kirkpatrick and Brow.[35] They explain this phenomenon according to the change in ionic

30 potential, i.e., the ratio of charge to radius of modifier cations; the NMR signals shift upfield as the ionic potential of the modifier cation increases. Because the ionic potential of proton is six times larger than that of Na^+ ion,[37] the ^{31}P NMR signals of the $HO_{1/2}$-$PO_{5/2}$ system appear upfield compared to those of the $NaO_{1/2}$-

35 $PO_{5/2}$ system even for the same Q^n unit, as summarized in Table 2.[38-41] Consequently, the observed upfield shift of the NMR signals of the glass after APS is because most Na^+ ions in the glass were substituted with protons during APS.

Based on the above explanation of the upfield shift of the ^{31}P

40 NMR signals after APS, the three signals of the glass after APS at -0.1, -14.8 and -28.0 ppm are assigned to Q^1, $Q^1_{(M)}$ and Q^2 units, respectively. The integrated intensity ratio of the signals arising from Q^2 and $Q^1_{(M)}$ units, $A_{Q^2}:A_{Q^1_{(M)}}$, of the glass before APS of 4.5:1, changed to 2.0:1 after APS. This suggests that APS

(a)

(b)

15

Fig.2 (a) Depth profiles of Na and OH concentrations measured by EDX and FTIR spectroscopies for 1W-glass after APS for 7 h. (b) Raman spectra of 1W-glass after APS for 7 h measured for the cross section along the direction from anode to cathode. x indicates the distance from

20   the anode.

(a)

(b)

45

Fig.3 ^{31}P MAS-NMR spectra of 1W-glass (a) before and (b) after APS for 30 h. Thin solid lines indicate the deconvoluted NMR signals assigned to Q^1, $Q^1_{(M)}$ and Q^2 units.

Table 2 Comparison of the 31P chemical shifts of sodium phosphate and phosphoric acid with various compositions.

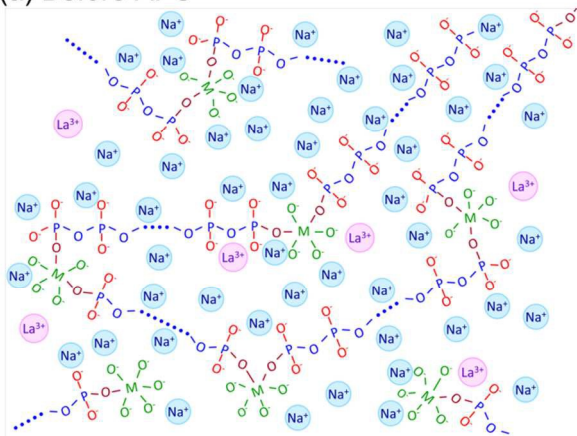| Material	PO$_4$ tetrahedra	Chemical shift (ppm)	Reference
Na$_3$PO$_4$	Q^0	13.7	38
H$_3$PO$_4$		0	
Na$_4$P$_2$O$_7$	Q^1	2.6	39
H$_4$P$_2$O$_7$		-11	40, 41
Na$_5$P$_3$O$_{10}$	Q^2	-5.6	39
H$_5$P$_3$O$_{10}$		-24.4	40, 41

induced fragmentation, that is, decreased the chain length m in $(PO_3^-)_m(P_2O_7^{4-})$, consistent with the results of Raman spectroscopy above.
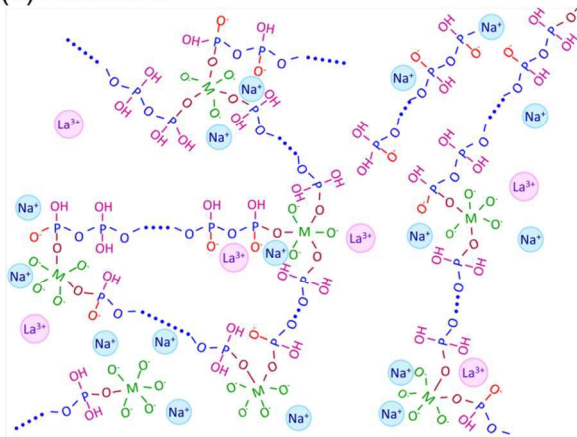
4. Discussion

4.1. Structure of the glass before APS

According to the results of Raman and NMR spectroscopies, the 1W-glass before APS consists of Q^1 and Q^2 units; for instance, the glass is mainly composed of $(PO_3^-)_m(P_2O_7^{4-})$ phosphate chains containing inner Q^2 units and two terminal Q^1 units. This

Fig.4 Schematic drawings of the structure of 1W-glass (a) before and (b) after APS.

structure is consistent with that expected based on the O/P ratio of the 1W-glass. The O/P ratio of the 1W-glass is 3.4, which is between that of pyrophosphate $(P_2O_7^{4-})$ of 3.5 and metaphosphate $(PO_3^-)_\infty$ of 3.0, even though the 1W-glass contains not only the simple modifier cations Na$^+$ and La^{3+} but also the intermediate cations W^{6+} and Nb^{5+}. Regarding WO$_3$ and NbO$_{5/2}$, the Raman spectrum clearly indicates the presence of MO$_6$ octahedra that have at least one NBO because stretching vibrations of ν_{MO} at 614 cm^{-1} and ν_{MO}^- at 924 cm^{-1} are both observed in the Raman spectrum (Fig. 1(a)).

Further quantitative information about the glass structure was deduced from the ^{31}P MAS-NMR spectrum of 1W-glass before APS as follows:
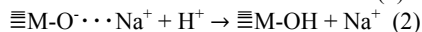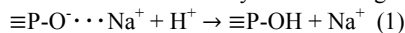
(i)   The structure of 1W-glass consists of only Q^1 and Q^2 units, without any other PO$_4$ units like Q^0 or Q^3.

(ii) The intensity ratio of $A_Q^1$$_{(M)}$:$A_Q^1$ was 18:1, which indicates that most of the terminal Q^1 units in $(PO_3^-)_m(P_2O_7^{4-})$ chains were bound to MO$_6$ octahedra.

(iii) The intensity ratio of A_Q^2:$(A_Q^1$$_{(M)}$ + $A_Q^1)$ was 4.3:1, indicating that the average formula of the phosphate chains is $(PO_3^-)_{8.6}(P_2O_7^{4-})$ assuming that the glass does not containing any pyrophosphate ions, $P_2O_7^{4-}$.

Based on these findings and the assumption that the Na$^+$ and La^{3+} ions as simple modifier ions compensate the negative charges of NBOs in PO$_4$ tetrahedral and MO$_6$ octahedral units, the structure of the 1W-glass before APS was deduced and is schematically illustrated in Fig. 4(a).

4.2. Structural changes induced by APS

1W-glass after APS is still composed of $(PO_3^-)_m(P_2O_7^{4-})$ phosphate chains. However, the length of the phosphate chains shortened slightly and the number of NBOs in each MO$_6$ octahedron was decreased by APS, i.e., APS in 1W-glass is not a simple and topotactic substitution of Na$^+$ ions with protons. The intensity ratios of the NMR signals of $A_Q^1$$_{(M)}$:$A_Q^1$ and A_Q^2:$(A_Q^1$$_{(M)}$ + $A_Q^1)$ were 9.4:1 and 1.84:1, respectively. These values indicate that the average formula of the phosphate chains in the glass after APS is $(PO_3^-)_{3.7}(P_2O_7^{4-})$ and most of the terminal Q^1 units in $(PO_3^-)_{3.7}(P_2O_7^{4-})$ chains still bond to MO$_6$ octahedra. Based on the fragmentation of the phosphate chains from $(PO_3^-)_{8.6}(P_2O_7^{4-})$ before APS to $(PO_3^-)_{3.7}(P_2O_7^{4-})$ after APS, and the formation of new M-O-P bonds instead of the consumption of some of the NBOs in the MO$_6$ octahedra during APS, the glass structure after APS was deducted and is schematically drawn in Fig. 4(b). Fragmentation of the phosphate-glass network usually occurs when the O/P ratio increases; *i.e.*, when the concentration of modifier cations increases. In the present case, the total number of modifier cations is the same before and after APS because the number of protons injected is the same as that of Na$^+$ ions discharged during APS.[13] However, some of the NBOs in the MO$_6$ octahedra before APS changed to BOs of the newly formed M-O-P bonds after APS. Consequently, the increased number of negative charges in the phosphate framework induced by fragmentation of the phosphate chain is compensated for by consumption of some of the NBOs in the MO$_6$ octahedra and formation of P-O-M bonds. The temperature used for APS (310 °C) was much higher than the glass transition temperature of the 1W-glass after APS (210 °C), so it seems reasonable that such a structural change could occur during APS. The structural

change observed during APS implies that the chemical driving force of this change originates from the preferential formation of P-OH bonds over M-OH bonds as follows: The positive charges of Na^+ ions in the glass before APS are compensated for by the negative charges of the NBOs in PO_4 tetrahedra ($\equiv$P-O$^-$) and MO_6 octahedra ($\equiv$M-O$^-$). During APS, Na^+ ions in the glass are substituted with protons and OH groups are formed in the glass, which can be described by the following reactions:

$$\equiv\text{P-O}^- \cdots Na^+ + H^+ \rightarrow \equiv\text{P-OH} + Na^+ \quad (1)$$

$$\equiv\text{M-O}^- \cdots Na^+ + H^+ \rightarrow \equiv\text{M-OH} + Na^+ \quad (2)$$

If the changes in energy for reactions (1) and (2) are comparable, Na^+ ions in the glass are simply substituted with protons and the glass network consisting of PO_4 tetrahedra and MO_6 octahedra does not change during APS. However, during APS, new M-O-P bonds are formed and the NBOs in MO_6 octahedra are consumed together with the fragmentation of the phosphate framework. This indicates that the following reaction (3) occurs instead of reaction (2) because of the difference in chemical bonding between Na^+ ions with NBOs and protons with oxygen atoms.

$$\equiv\text{M-O}^- \cdots Na^+ + \equiv\text{P-O-P}\equiv + H^+ \rightarrow \equiv\text{M-O-P}\equiv + \equiv\text{P-OH} + Na^+ \quad (3)$$
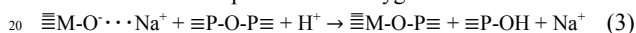
This suggests that the formation of $\equiv$M-O-P$\equiv$ and $\equiv$P-OH is favored rather than the formation of $\equiv$M-OH under the conditions, *i.e.*, temperature and atmosphere, used for the present APS, and may be mainly caused by $\equiv$P-OH being more stable than $\equiv$M-OH under these conditions. Because of this, most protons injected into the glass are trapped by PO_4 tetrahedra and form $\equiv$P-OH bonds, so almost no $\equiv$M-OH bonds exist in the glass after APS. The formation of $\equiv$M-O-P$\equiv$ in the glass after APS may not be favored in terms of the stability. When the formation of $\equiv$M-O-P$\equiv$ bonds heavily develops, the phase separation into $NbO_{5/2}$ or WO_3 and $PO_{5/2}$ rich phase and the other phase is much-feared.

Under the present APS conditions (310 °C and applied DC voltage of 5V), some Na^+ ions were not substituted with protons and remained in the glass after APS, as shown in Fig. 5(a) and described in our previous paper.[13] The composition of the glass after APS is expressed as $11NaO_{1/2}$-$24HO_{1/2}$-$1WO_3$-$8NbO_{5/2}$-$5LaO_{3/2}$-$51PO_{5/2}$. The Raman spectrum of the glass after APS (Fig. 1(b) and Table 1) indicates that the NBOs in MO_6 octahedra remain in the glass after APS; therefore, the negative charges of these NBOs must be compensated for by not protons but Na^+ and/or La^{3+} ions. This suggests that the Na^+ ions left in the glass after APS, which should possess lower mobility than that of the Na^+ ions discharged out of the glass, exist around the MO_6 octahedra. We attempted to discharge all Na^+ ions in the $30NaO_{1/2}$-$1WO_3$-$8NbO_{5/2}$-$5LaO_{3/2}$-$56PO_{5/2}$ glass and to inject protons by APS under application of 10 V of DC voltage. The resulting glass was highly hygroscopic indicating the formation of hygroscopic $PO_{5/2}$-rich phase by phase separation; therefore, the glass was not enough to be subjected to various analyses. This phase separation should be induced by that the NBOs in MO_6 octahedra compensated by Na^+ ions transformed into BO according to the reaction (3) and $\equiv$M-O-P$\equiv$ bonds were highly developed in the glass after APS. This strongly suggests that it would be better for the concentrations of $NbO_{5/2}$ and WO_6 in the glass not to be high in terms of the stability of the glass.

5. Conclusions

The structures of 1W-glass, $1WO_3$-$35NaO_{1/2}$-$8NbO_{5/2}$-$5LaO_{3/2}$-$51PO_{5/2}$, before and after APS were studied in detail by Raman and ^{31}P MAS-NMR spectroscopies. The glass network of 1W-glass before APS consists mainly of $(PO_3^-)_m(P_2O_7^{4-})$ chains with m=8.6 on average and the terminal Q^1 units are bound to NbO_6 or WO_6 octahedra through P-O-Nb or P-O-W bonds. There are some NBOs in the NbO_6 and WO_6 octahedra in addition to the BOs in P-O-Nb or P-O-W bonds. APS induces fragmentation of the phosphate chains because the average length decreases from $(PO_3^-)_{8.6}(P_2O_7^{4-})$ before APS to $(PO_3^-)_{3.7}(P_2O_7^{4-})$ after APS, even though the total number of modifier cations of Na^+ and La^{3+} ions and protons is not changed by APS. The fragmentation of the phosphate framework is induced by some of the NBOs in the MO_6 octahedra before APS changing to BOs of the newly formed M-O-P bonds during APS. The structural change during APS arises from the preferential formation of P-OH bonds over M-OH bonds. As a result, APS is not a simple and topotacitic substitution of Na^+ ions with protons but is accompanied with structural relaxation to stabilize the injected protons. Formation of M-O-P bonds during APS may not be favored in terms of the stability of the glass, because the phase separation into $NbO_{5/2}$ or WO_3 and $PO_{5/2}$ rich phase and the other phase is much-feared when the formation of $\equiv$M-O-P$\equiv$ bonds heavily develops. Further, fragmentation of the phosphate framework generally leads to a decrease of the glass transition temperature. Therefore, it is important to design a glass composition where phase separation and fragmentation of the glass network does not occur during APS to realize proton-conducting glass electrolytes with high thermal stability suitable for use as the electrolyte of ITFCs.

Notes

a Division of Materials and Manufacturing Science, Graduate School of Engineering, Osaka University, 2-1 Yamada-oka, Suita 565–0871, Japan
b Research Institute for Electronic Science, Hokkaido University, Kita 21 Nishi 10, Kita-ku, Sapporo 001-0021, Japan
c Kawazoe Frontier Technologies Corp., Kuden-cho 931-113, Sakae-ku, Yokohama 247-0014, Japan
d Institute of Multidisciplinary Research for Advanced Materials, IMRAM Tohoku University, Katahira 2-1-1, Aoba-ku, Sendai 980-8577, Japan
† Present address: Fuel Cell Materials Group, Research Institute for Energy Conservation, National Institute of Advanced Industrial Science and Technology (AIST), AIST Central 5, Higashi 1-1-1, Tsukuba, Ibaraki 305-8565, Japan
* Corresponding author. Tel: +81-6879-7462; Fax: +81-6879-7464.
E-mail: omata@mat.eng.osaka-u.ac.jp

References

1   D. J. L. Brett, A. Atkinson, N. P. Brandon and S. J. Skinner, *Chem. Soc. Rev.,* 2008, **37**, 1568.
2   B. Zhu, *J. Power Sources,* 2001, **93**, 82.
3   J. P. P. Huijsmans, F. P. F. Berkel and G. M. Christie, *J. Power Sources,* 1998, **71**, 107.
4   T. Norby, *Solid State Ionics,* 1999, **125**, 1.
5   E. D. Wachsman and K. T. Lee, *Science,* 2011, **334**, 935.
6   J. Huang, F. Xie, C. Wang and Z. Mao, *Int. J. Hyd. Eng.,* 2012, **37**, 877.

7   E. Fabbri, D. Pergolesi and E. Traversa, *Chem. Soc. Rev.,* 2010, **39**, 4335.

8   E. Fabbri, L. B. D. Pergolesi and E. Traversa, *Adv. Mater.,* 2012, **24**, 195.

9   H. Iwahara, H. Uchida, K. Ono and K. Ogaki, *J. Electrochem. Soc.,* 1988, **135**, 529.

10   D. A. Boysen and S. M. Haile,*Chem. Mater.,* 2003, **15**, 727.

11   T. Ishiyama, S. Suzuki, J. Nishii, T. Yamashita, H. Kawazoe and T. Omata, *J. Electrochem. Soc.,* 2013, **160**, E143.

12   T. Ishiyama, S. Suzuki, J. Nishii, T. Yamashita, H. Kawazoe and T. Omata, *Solid State Ionics,* 2014, **262**, 856.

13   T. Ishiyama, J. Nishii, T. Yamashita, H. Kawazoe and T. Omata, *J. Mater. Chem. A,* 2014, **2**, 3940.

14   P. Vinatier, M. Ménétrier and A. Levasseur, *Solid State Ionics*, 1999, **116**, 35.

15   J. Saienga and S.W. Martin, *J. Non-Cryst. Solids*, 2008, **354**, 1475.

16   I. Svare, F. Borsa, D.R. Torgeson and S.W. Martin, *Phys. Rev. B*, 1993, **48**, 9336.

17   Y. Abe, H. Shimakawa, and L. Hench, *J. Non-Cryst. Solids*, 1982, **51**, 357-365.

18   Y. Abe, G. Li, M. Nogami and T. Kosuga, *J. Electrochem. Soc.,* 1996, **143**, 144.

19   G. C. Farrington, J. L .Briant, M. W. Breiter and W. L. Roth, *J. Solid State Chem.*, 1978, **24**, 311.

20   J.D. Denuzzio and G.C. Farrington, *J. Solid State Chem.,* 1989, **79**, 65.

21   A. Kuhn, H. Bashir, A. L. Dos Santos, J. L. Acosta and F. García-Alvarado, *J. Solid State Chem.*, 2004, **177**, 2366.

22   T. Yamaguchi, T. Ishiyama, K. Sakuragi, J. Nishii, T. Yamashita, H. Kawazoe, T. Omata, *Solid State Ionics*, in press.   doi: 10.1016/j.ssi.2015.03.003

23   D. Massiot, F. Fayon, M. Capron, I. King, S. Le Calvé, B. Alonso, J.-O. Durand, B. Bujoli, Z. Gan and G. Hoatson, *Magn. Reson. Chem.,* 2002, **40**, 70.

24   M. G. Donato, M. Gagliardi, L. Sirleto, G. Messina, A. A. Lipovskii, D. K. Tagantsev and G. C. Righini, *Appl. Phys. Lett.,* 2010, **97**, 231111.

25   K. Fukumi and S. Sakka, *J. Mater. Sci.,* 1988, **23**, 2819.

26   A. EL. Jazouli, J. C. Viala, C. Parent, G. LE Flem and P. Hagenmuller, *J. Solid State Chem.,* 1988, **73**, 433.

27   J. M. Jehng and I. E. Wachs, *Chem. Mater.,* 1991, **3**, 100.

28   R. K. Brow, *J. Non-Cryst. Solids,* 2000, **263-264**, 1.

29   R. K. Brow, D. R. Tallant, J. J. Hudgens, S. W. Martin and A. D. Irwin, *J. Non-Cryst. Solids,* 1994, **177**, 221.

30   M. Tatsumisago, Y. Kowada and T. Minami, *Phys. Chem. Glasses,* 1988, **29**, 63.

31   J. E. Pemberton and L. Latifzadeh, *Chem. Mater.,* 1991, **3**, 195.

32   D.A.Long, *Raman Spectroscopy*, McGraw-Hill, New York, 1977, pp80-87.

33   A. Derevianko, W. R. Johnson, M. S. Safronova and J. F. Babb, *Phys. Rev. Lett.,* 1999, **82**, 3589.

34   S.P. Goldman, *Phys. Rev. A*, 1989, **39**, 976.

35   R. J. Kirkpatrick and R. K. Brow, *Solid State Nucl. Magn. Reson.,* 1995, **5**, 9.

36   C. C. Araujo, W. Strojek, L. Zhang, H. Eckert, G. Poirier, S. J. L. Ribeiro and Y. Messaddeq, *J. Mater. Chem.,* 2006, **16**, 3277.

37   G. H. Cartledge, *J. Am. Chem. Soc.,* 1928, **50**, 2855.

38   S. Prabhakar, K. J. Rao and C. N. R. Rao, *Chem. Phys. Letters,* 1987, **139**, 96.

39   S. Hayashi and K. Hayamizu, *Chem. Phys.,* 1991, **157**, 381.

40   M. M. Crutchield, C. F. Callis, R. R. Irani and G. C. Roth, *Inorg. Chem.,* 1962, **1**, 813.

41   S. H. Chung, S. Bajue and S. G. Greenbaum, *J. Chem. Phys.,* 2000, **112**, 8515.